



**Michigan
Technological
University**

Michigan Technological University
Digital Commons @ Michigan Tech

Department of Physics Publications

Department of Physics

5-1-1999

Non-Rayleigh signal statistics in clustered statistically homogeneous rain

A. R. Jameson
RJH Scientific, Inc.

Alexander Kostinski
Michigan Technological University

Follow this and additional works at: <https://digitalcommons.mtu.edu/physics-fp>



Part of the [Physics Commons](#)

Recommended Citation

Jameson, A. R., & Kostinski, A. (1999). Non-Rayleigh signal statistics in clustered statistically homogeneous rain. *Journal of Atmospheric and Oceanic Technology*, 16(5), 575-583. [http://dx.doi.org/10.1175/1520-0426\(1999\)016<0575:NRSSIC>2.0.CO;2](http://dx.doi.org/10.1175/1520-0426(1999)016<0575:NRSSIC>2.0.CO;2)
Retrieved from: <https://digitalcommons.mtu.edu/physics-fp/252>

Follow this and additional works at: <https://digitalcommons.mtu.edu/physics-fp>



Part of the [Physics Commons](#)

Non-Rayleigh Signal Statistics in Clustered Statistically Homogeneous Rain

A. R. JAMESON

RJH Scientific, Inc., Alexandria, Virginia

A. B. KOSTINSKI

Department of Physics, Michigan Technological University, Houghton, Michigan

(Manuscript received 17 February 1998, in final form 28 July 1998)

ABSTRACT

As the sample volume of a remote sensing instrument moves through sufficiently variable conditions, recent work shows that the amplitudes and associated intensities can deviate significantly at times from expectations based on Rayleigh signal statistics because fluctuations in the number of scatterers leads to a doubly stochastic measurement process. While non-Rayleigh deviations yield average biases for both logarithmic and linear detectors, perhaps of greater importance is the enhancement of the variance of the bias distribution for square law detectors. In this work the authors explore the potential existence of non-Rayleigh effects even in the statistically homogeneous rain when fluctuations in the number of scatterers should be much less than for the inhomogeneous conditions used in earlier studies.

Moreover, in contrast to previous work, recent advances now permit the simulation of correlated rainfall structures having the statistical characteristics of natural rain such as clustering intensity (\aleph) and coherence length (χ_l) consistent with observations. The primary objective of this work, then, is to clarify how \aleph , χ_l , and the geometric parameters characteristic of remote sensing observations such as the distance over which an estimate is made (L), the beamwidth (B), and the spatial displacement between successive independent samples (Δ) affect non-Rayleigh signals statistics in statistically homogeneous rain.

This work shows that non-Rayleigh effects can appear whenever $\Delta \leq \chi_l \leq L$. Moreover, the magnitudes of the non-Rayleigh deviations increase as \aleph and Δ/B increase. Although non-Rayleigh effects can be detected by monitoring of the signals, keeping both Δ/B and L as small as possible while increasing sample independence using chirp or signal whitening techniques, for example, should help to minimize non-Rayleigh effects for radars even in statistically inhomogeneous rain.

1. Introduction

The assumption of Rayleigh statistics is a main stay in much of remote sensing. The work of Lord Rayleigh (1877) was extended to radar by Marshall and Hitschfeld (1953) and subsequently expounded by many including Doviak and Zrnić (1993) most recently. Rayleigh statistics, however, are based upon the Central Limit Theorem applied to each of the two components of the complex signal when conditions are “near” statistical stationarity. Jameson and Kostinski (1996) explored the meaning of near stationarity and concluded, for the simple case of drops of one size, that whenever the number of “drops” within the beam fluctuated from sample to sample by more than about 15% of the mean, non-Rayleigh effects could be detected. Why? Because now the measurement not only depends upon the constructive

and destructive interference of the waves scattered off all the drops, it also depends upon the doubly stochastic nature of the process (see Feller 1968, 53 for a discussion on randomization and mixtures) in which the number of scatterers themselves becomes a random variable largely because of the motion of the observation volume between successive radar samples. These conclusions have been substantiated using Monte Carlo experiments of a radar beam moving across a linear gradient of the logarithm of Z (Jameson and Kostinski 1996) consistent with measurements (Schaffner et al. 1980; Schaffner et al. 1983; Scarchilli et al. 1986).

While these latter simulations support the theory, they are limited in two respects. Specifically, by simply imposing linear gradients of the logarithm of Z , it becomes impossible to relate the presence and magnitudes of non-Rayleigh effects to actual, natural rain structure characterized by properties such as correlation length and clustering intensity. Furthermore, had such gradients been arbitrarily set to zero, non-Rayleigh effects could not exist in the resultant spatially uniform rain. However, because rain is a stochastic quantity, it never ex-

Corresponding author address: A. R. Jameson, 5625 N. 32nd St., Arlington, VA 22207.
E-mail: jameson@rjhsci.com

hibits true spatial uniformity but instead is uniform only in the sense that it can be statistically homogeneous. Even with this understanding, however, for convenience it is frequently assumed that raindrops are distributed according to Poisson statistics, the most “even” spatial (and temporal) distribution of drops. Recent studies, however, show that while such an assumption may occasionally be valid in unusually steady rain (Kostinski and Jameson 1997), the Poisson distribution utterly fails to describe accurately the spatial structure and drop concentration fluctuations of natural, variable rain (Kostinski and Jameson 1997; Kostinski and Jameson 1999; Jameson et al. 1999).

The reason is that most variable rain is “clustered,” that is, the physical variations in concentration (number per unit volume) exceed those anticipated for a Poisson distribution. To demonstrate what is meant by clustered raindrops, one begins with the product of the number of drops in two identical volumes separated by a fixed distance, ξ , and then subtracts the square of the average value computed over the entire volume under study, \mathcal{V} , for an ensemble of several such pairs in \mathcal{V} . That is, we consider the quantity

$$\phi(\xi) = \langle k(0)k(\xi) \rangle - \mu^2, \quad (1)$$

where $k(0)$ and $k(\xi)$ are the number of drops in two identical volumes separated by distance ξ , μ is the mean number over all of \mathcal{V} , and the brackets denote an ensemble average over many pairs. If the number of drops in \mathcal{V} are distributed evenly on average, then $\langle k(0)k(\xi) \rangle = \mu^2$ so that $\phi(\xi) = 0$. If, on the other hand, there were an “excess” number of drops in volumes separated by scales of ξ on average, $\phi(\xi)$ would not equal zero, that is, $[\langle k(0)k(\xi) \rangle] \neq \mu^2$. In other words, there would be a clustering of drops compared to the average number expected for a uniform, statistical spatial (Poisson) distribution over \mathcal{V} .

The statistical interpretation of (1) given in Kostinski and Jameson (1997) is in terms of the *excess* two-point correlation function given by

$$\begin{aligned} \eta(\xi) &= \frac{[\langle k(0)k(\xi) \rangle - \mu^2]}{\mu^2} \\ &= \frac{\langle k(0)k(\xi) \rangle}{\mu^2} - 1. \end{aligned} \quad (2)$$

For a Poisson distribution, $k(0)$ and $k(\xi)$ would be statistically independent. Consequently, $\langle k(0)k(\xi) \rangle = \mu^2$ and $\eta(\xi) = 0$ even though k fluctuates from location to location. However, when $\eta(\xi) \neq 0$ there is correlation. Hence, according to Kostinski and Jameson (1997), it is the statistical correlation of drops in one volume on the presence of drops in another that distinguish clustering from a uniform Poisson distribution.

To illustrate, Fig. 1 is a plot of $\eta(\xi)$ estimated from 1-s temporal drop counts (Jameson et al. 1999) in a 3-min convective rain. An arbitrary distance scale is calculated assuming a mean translation speed of 2 m

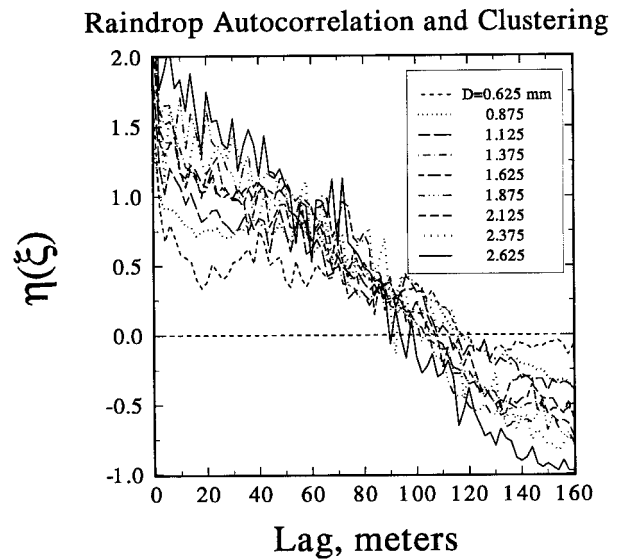


FIG. 1. The two-point autocorrelation function calculated for drop counts per second for the indicated drop sizes for a 201-s rain event observed by a video disdrometer. Time has been converted to distance assuming a translation speed of 2 m s^{-1} . The dashed line at zero indicates complete statistical independence as expected for a Poisson distribution. Note the enhanced clustering even down to the 1-s (2 m) lag.

s^{-1} . Had the distributions been Poisson, $\eta(\xi)$ would be zero (Kostinski and Jameson 1997). Instead there is significant drop clustering. While the reader is referred to Kostinski and Jameson (1997) for a more complete statistical description of clustering, Fig. 1 serves to highlight two important quantities.

The first is $\aleph \equiv \sigma^2/\mu^2[1 - \mu/\sigma^2] = \eta(0)[1 - \mu/\sigma^2]$ where μ and $\sigma^2(k)$ are the mean and variance, respectively, of the number (counts) of drops in a unit volume averaged over the entire observation. Thus, for Poisson distributions, when there is no clustering, $\aleph \rightarrow 0$, because $\sigma^2 = \mu$. On the other hand, when clustering is occurring, as described by the geometric distribution for example, then $\aleph \rightarrow \eta(0)[\mu/(1 + \mu)] \rightarrow 1$ as can be readily seen by substituting $\eta(0) = \sigma^2/\mu^2$ and by noting that for the geometric distribution $\sigma^2 = \mu + \mu^2$. In fact for other negative binomial distributions, it is easy to show that $\aleph \rightarrow \eta(0)[\mu/(m + \mu)] \rightarrow 1/m$ as $\xi \rightarrow 0$, where m is the so-called shape parameter of the gamma distribution transformed into a negative binomial distribution by the Poisson mixture process (for elaboration see Kostinski and Jameson 1997, 2177–2178). Consequently, the larger the \aleph , the smaller the m . Because of the nature of the gamma distribution, this in turn means that as \aleph increases, m decreases and the resulting shape of the distribution of drop counts per unit volume changes such that the tail of the distribution extends to larger counts; simultaneously, the probability densities at small values near zero also increases. This, of course, is what is meant by the increased clustering or clumping of raindrops. That is, there are simultaneously both more

regions of lower concentrations of drops and more regions of higher drop concentrations, that is, clusters. Hence, as \aleph increases, the clustering of the raindrops increases.

The second quantity is the coherence length χ_l , which is the distance at which $\eta(\chi_l)$ becomes negligible. This latter quantity then provides a measure of the average scale or size of the clusters. These two variables (χ_l and \aleph) are important because they provide a way of characterizing clustering and, therefore, of generating realistic structures of rain numerically even for statistically homogeneous rain. Hence, we can now explore the relation between χ_l and \aleph (i.e., clustering) and radar sampling even in statistically homogeneous rain, a task not possible in previous studies.

Specifically, in this study we describe a method for generating realistic rain structures having different χ_l and \aleph . We identify the “geometric” scales important to the observations as well as how the geometry and spatial characteristics of the rain interact to yield non-Rayleigh effects even in statistically homogeneous rain. In addition, we briefly consider how correlated radar samples increase the likelihood of non-Rayleigh effects. Finally, using these results we suggest approaches for minimizing potential non-Rayleigh effects for radars and for other remote sensing instruments as well.

2. Monte Carlo simulations of radar measurements in clustered rain

It is now well established in variable rain that drop counts deviate from Poisson statistics and are often well approximated by the geometric distribution (Kostinski and Jameson 1999; Jameson et al. 1999). While it is possible to readily generate uncorrelated pseudorandom deviates of drop counts for Monte Carlo simulations using a geometric distribution (e.g., Evans et al. 1993), an important property of variable rain is that the drop counts are *correlated* in time and space as just discussed. In fact, drop concentrations in variable rain are usually correlated not only at one size but also among sizes (Jameson and Kostinski 1998). However, to reduce the complexity of this study, we use only one drop size D_z that represents the diameter contributing most to the radar reflectivity factor (see Jameson and Kostinski 1996). Correlations even at one drop size, however, are important because they introduce larger-scale structures even in statistically homogeneous rain, thereby increasing the likelihood of non-Rayleigh effects (changing number of scatterers during sampling).

Before conducting Monte Carlo simulations of a radar scanning clustered rain, it is necessary first to describe briefly the generation of correlated rain samples having variable χ_l and \aleph . We then identify scales important to sampling, and we describe the Monte Carlo radar sampling procedure. In later sections, simulation results are presented and discussed.

a. Generation of realistic correlated rain structures

While there are several techniques in the literature for generating correlated samples, one of the more rigorous approaches, and the one used in this study, is that given by Johnson (1994). Although details may be found in that work, the approach is described here very briefly.

Beginning with a family of exponential correlation functions having different χ_l , the correlation matrix is constructed. The root matrices for these correlation matrices are computed and then multiplied by a series of zero mean, unit variance random deviates drawn from the geometric probability density function (PDF). The variance of this series is then adjusted to yield the desired \aleph , and the mean value is added to yield the final correlated series of statistically homogeneous drop concentrations.

To illustrate these results, Fig. 2a is a plot of $\eta(l)$ [Eq. (2)] for the family of correlation functions used in this study. In good agreement with observations (Fig. 1), this plot shows that we have successfully generated clustered rain over a wide range of correlation lengths and with values of \aleph near unity. (Observed values of \aleph typically range from 0.5 to 2.5 but on some occasions may achieve values as large as 6 or greater.) Furthermore, Fig. 2b illustrates that the simulated PDFs are also quite geometric.

The results can also be displayed as a series (Fig. 3a) having a mean value of $\mu = 355$ drops of 2-mm diameter per cubic meter for two different χ_l 's as a function of unitless distance. (Throughout this work, the dimensions and distance are kept unitless, but the reader may multiply by any comfortable value.) In this figure, the region of rain to be scanned by the radar in the Monte Carlo simulations is denoted by the shading. The corresponding radar reflectivity factor series is also shown in Fig. 3b for a 10-unit-wide beam. These structures can be assumed fixed for most remote sensing measurements. That is, the correlation times of the structures are considerably longer [several seconds to minutes (Jameson and Kostinski 1998; Jameson et al. 1999)] than the fraction of a second it usually takes a radar to make an estimate. (This structure coherence time, however, should not be confused with the much shorter “time to independence” as the scatterers reshuffle phase during sampling.) While the shaded region in Fig. 3a was selected to provide a large signal, such fluctuations of this magnitude are a characteristic of the geometric distribution for which the variance scales as μ^2 rather than simply μ as for the Poisson distribution. Hence, this region is not especially peculiar nor are such fluctuations a rare occurrence in natural spatial distributions of raindrops (e.g., see the variances in Fig. 6 in Kostinski and Jameson 1997 and Fig. 2 in Jameson et al. 1999).

b. Radar scales and scanning

As illustrated in Fig. 4, when sampling by a remote sensing instrument such as radar, there are three scales

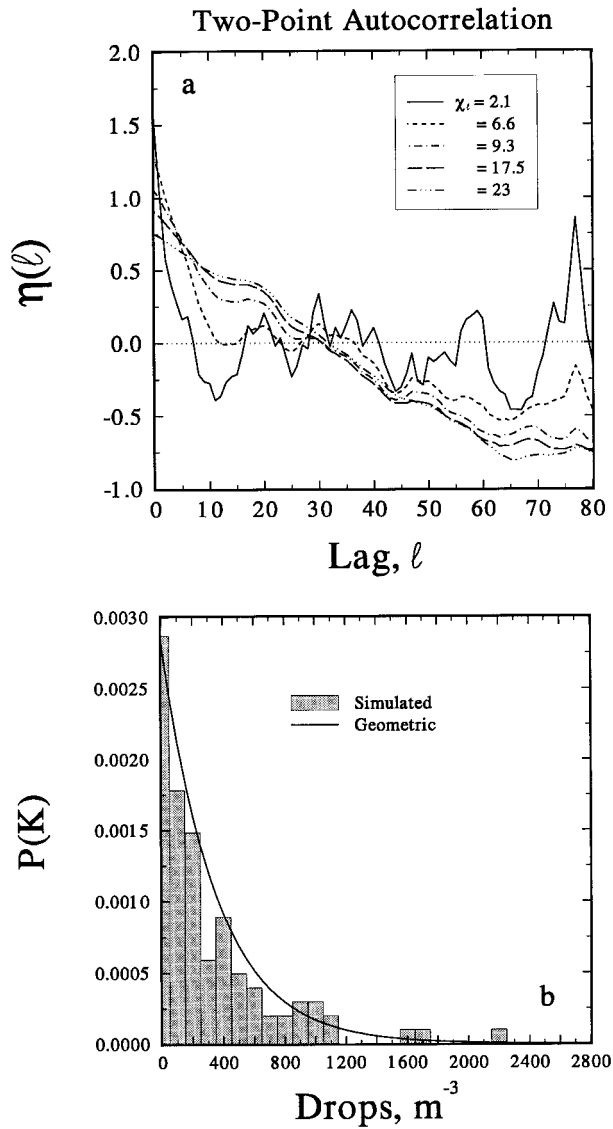


FIG. 2. (a) The two-point autocorrelation functions calculated for the Monte Carlo simulations discussed in the text corresponding to exponential correlation functions with the indicated coherence ($1/e$) distance, χ_l . The distances are unitless as discussed in the text. (b) A comparison between simulated and geometric probability density functions for $\chi_l = 9.3$ and $\aleph = 1$.

of the measurement, namely the beam dimension B , the incremental distance the beam moves between independent samples Δ , and the total measurement length associated with an estimate derived from n samples, $L = n\Delta$. What we will explore in this work is the relationship of these quantities and their effects on signal statistics to the intrinsic characteristics of the rainfall structure, namely, the correlation length χ_l and the clustering intensity \aleph as discussed above.

For linear and logarithmic detectors, an important effect of non-Rayleigh statistics is a deviation of the measured mean value from Rayleigh expectations. However,

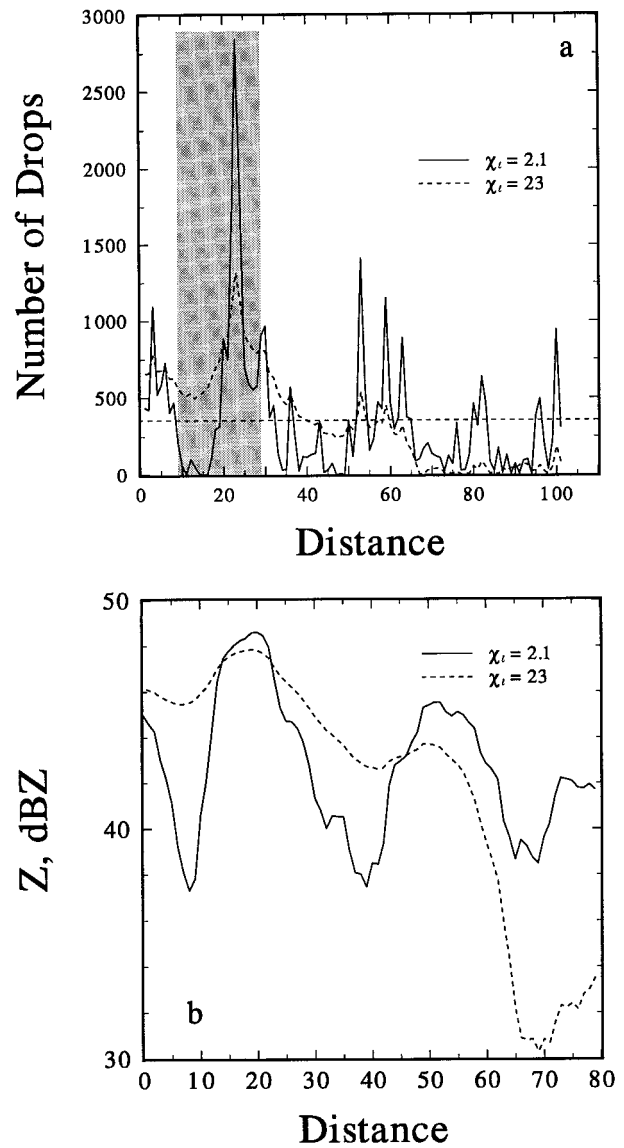


FIG. 3. (a) The number N_z of $D_z = 2$ mm drops per cubic meter as a function of unitless distance for two coherence distances and for correlated drop counts drawn from one realization of a geometric distribution. The shaded region denotes where radar measurements were simulated for subsequent analyses, while the horizontal line denotes the mean, μ . (b) Plots of the radar reflectivity factor $N_z D_z^6$ as "observed" by a 10-unit-wide beam corresponding to (a).

for square law detectors this mean is unbiased so that it is the non-Rayleigh enhancement of the variance σ^2 of the bias PDF that becomes most important, as pointed out in Jameson and Kostinski (1996). (For logarithmic and linear detectors, there may actually be a narrowing of the bias PDF, but then there are also simultaneous significant bias shifts of the mean, unlike the case for a square law detector.) While for completeness we illustrate the mean biases with regard to logarithmic and linear detectors, our chief concern here is the enhancement of the variance of the bias for so-called unbiased

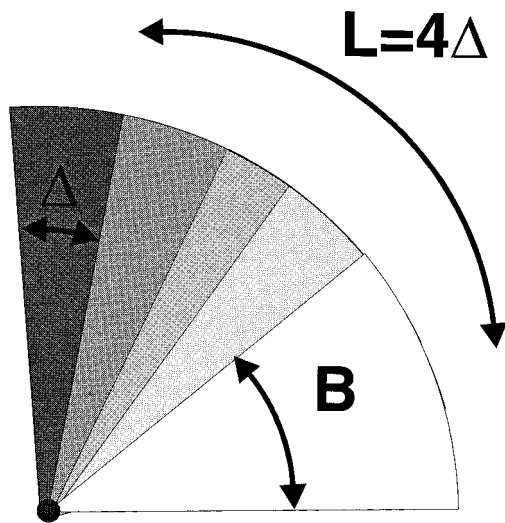


FIG. 4. A schematic diagram defining the distance between successive statistically independent pulses Δ , the beam width B , and the distance L associated with an estimate calculated from many samples.

square law detectors. Why? Because normally a radar makes only one pass across a region before conditions change. Hence, a particular estimate can be viewed as just one draw from the bias PDF, a distribution that is different by the time the radar returns for another look usually several minutes later. Therefore, any increase in σ^2 due to non-Rayleigh effects then increases the uncertainty associated with that one particular estimate.

To determine the effects of this bias PDF on measurements, and its relation to rain structure and measurement geometry, we perform a series of Monte Carlo experiments. Specifically, we scan a beam across the shaded region in Fig. 3a several thousand times in order to extract not only reliable estimates of mean bias, but as importantly, reliable estimates of the variance enhanced beyond that anticipated for Rayleigh statistics. To do this we consider a uniformly illuminated beam 10 units wide ($B = 10$). At each point in Fig. 3a the drop concentration is converted into radar reflectivity factor Z_i simply by multiplying $D_z = 2$ mm raised to the sixth power times the number of drops per cubic meter, as illustrated in Fig. 3b. For each radar sample, a random phasor P_i is generated at each of the 10 points in the beam having a magnitude drawn from a Rayleigh PDF consistent with each Z_i but with a random phase uniformly distributed over 0 to 2π . These 10 P_i 's are then vector summed and the intensity is determined using the three different detectors, namely, the square law, linear (amplitude), and logarithmic receivers. The beam is then subsequently moved by $\Delta = N$ points ($1 \leq N \leq 9$) and a new sample is made. Because of the random distribution of phase, each sample is statistically independent in a manner analogous to chirping the radar frequency between from pulse to pulse. Finally, the samples are averaged to yield an estimate over L . Since we

know the true mean value of the statistically homogeneous rain, 20 000 such realizations are then used to calculate the observed mean bias and bias variance for the three different detectors. The results of a series of experiments are discussed in the next section.

3. Results

In the first series of experiments, we let $B = 10$, $\Delta = 0.1B$, and $k_i = 10$, where k_i is the number of independent samples so that Δ is the spatial separation between independent samples. The results for the mean biases as functions of χ_i/L are plotted in Fig. 5a. As expected (e.g., Jameson and Kostinski 1996), the mean bias for the square law detector is unaffected by clustering, while there are small but real deviations approaching 1 dB for both the log and linear receivers. Again, however, it is important to remember that for square law detectors the mean is not a very useful parameter for characterizing the bias PDF. Rather, the more relevant quantity is the standard deviation of the PDF, as illustrated in Fig. 5b. Note that both the mean biases and standard deviations (σ) approach the Rayleigh limit as the correlation length exceeds the estimate distance, that is, $\chi_i/L \geq 1$. This is consistent with the "patch" characterization of rain (Kostinski and Jameson 1997). That is, within a patch the raindrop statistics should be Poisson (i.e., there should be no clustering on average). Thus, as long as L , the distance associated with an estimate, is less than the size of a patch, Rayleigh signal statistics should apply. On the other hand, as $\chi_i < L$, there is mixing of measurements from several patches so that the raindrop statistics deviate from Poisson. The result is clustering, and non-Rayleigh effects begin to appear as Fig. 5 illustrates. Note, however, that in this particular case as $\chi_i \rightarrow 0$, the values do not go to the Rayleigh limit because the beam still acts to correlate fluctuations across the beam, that is, it averages all the fluctuations across the beam simultaneously from sample to sample contributing to the estimate. On the other hand, had there been, say, 1000 points in B instead of the 10 as in this example, then the curves might well approach the Rayleigh limit as $\chi_i \rightarrow 0$.

While the above example shows that non-Rayleigh deviations depend upon χ_i/L , we next illustrate that their magnitudes also depend upon \aleph , the clustering intensity. In particular let $\chi_i/L = 0.2$, $\Delta = 0.1B$, $k_i = 10$, and $L = 10$. Then as Fig. 6 illustrates, deviations from Rayleigh expectations increase with increasing \aleph . This, of course, makes sense because the larger the \aleph , the greater the clustering. Consequently, there will be larger fluctuations in drop concentrations, greater fluctuations in the radar reflectivity factor, and hence larger deviations from Rayleigh statistics. Thus, while the results in Fig. 5 are for $\aleph \sim 1$, observations (Kostinski and Jameson 1997; Jameson and Kostinski 1999) suggest that $2 \leq \aleph \leq 8$ may not be uncommon, particularly in the cores of convective storms. If this is so, then the potential

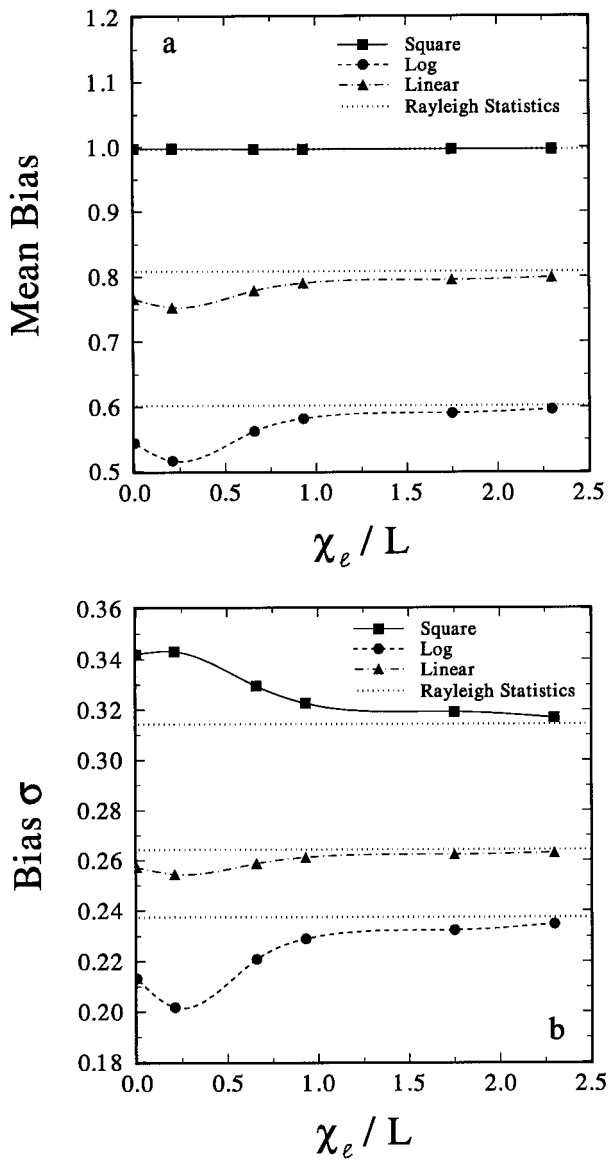


FIG. 5. (a) The average biases and (b) associated standard deviations of the bias probability density functions (PDFs) as functions of χ_e/L in statistically homogeneous rain computed from 20 000 realizations of radar measurements over the shaded region in Fig. 3 assuming $B = 10$, $\Delta = 0.1B$, and $L = B$ and 10 independent samples for square law, logarithmic, and linear detectors. The variable \aleph is near unity. The dashed lines denote values expected for Rayleigh statistics.

effects of clustering on signals even in statistically homogeneous rain may be enhanced beyond the results shown in Fig. 5.

Moreover, non-Rayleigh effects also depend upon the ratio of the distance between independent samples to the beam width, (Δ/B), as illustrated in Fig. 7 for $\chi_e/L = 0.2$, $k_i = 10 = \text{constant}$ and $L = B = 10$. As one might anticipate, deviations in the mean bias and σ increase with increasing Δ/B . This is sensible because as

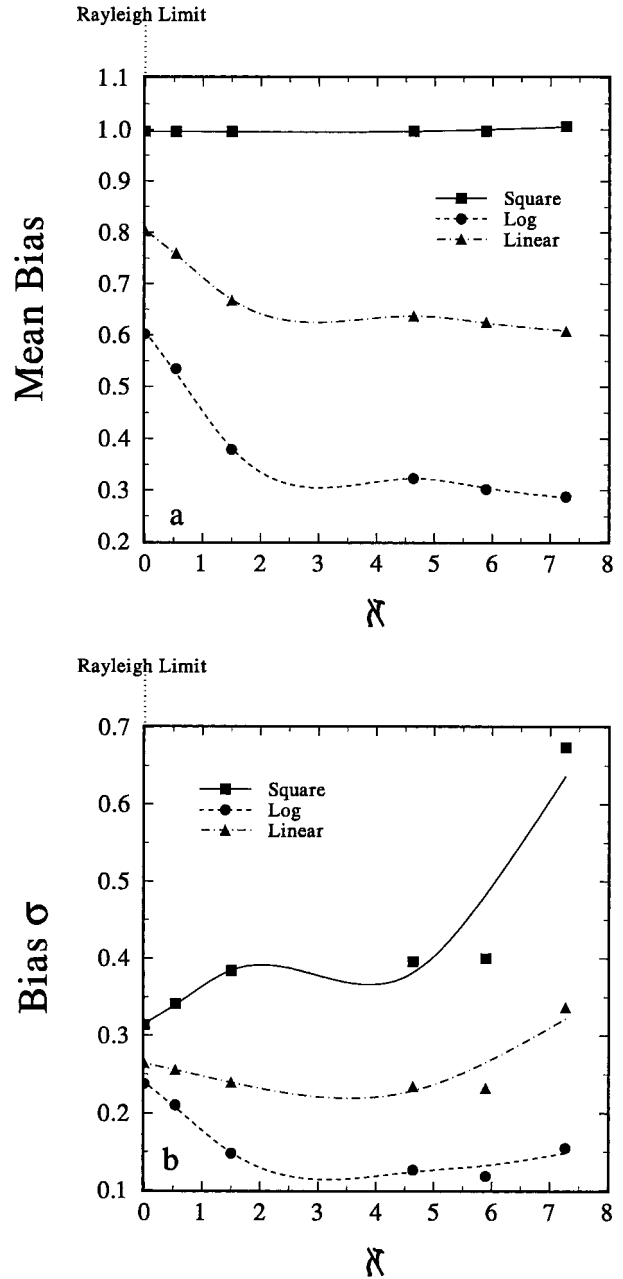


FIG. 6. (a) Values of the mean biases and (b) standard deviations of the bias PDFs in statistically homogeneous, clustered rain as functions of the clustering intensity \aleph , as described in the text.

Δ increases there are likely to be greater changes in the rain field (decorrelation) and, therefore, greater differences in the number of scatterers from sample to sample. However, Fig. 7 is somewhat misleading in that it assumes that the number of independent samples is somehow kept constant. In practice that would not be likely. Often the pulse repetition frequency is maintained even as the antenna rotation rate is increased. Consequently, the interval Δ between independent samples would usu-

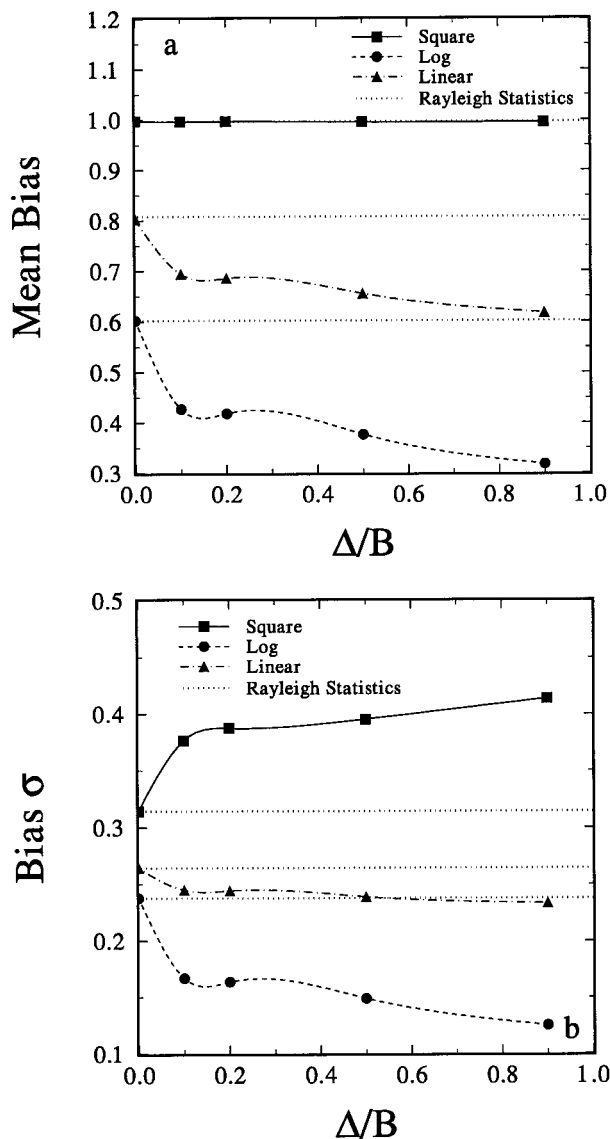


FIG. 7. (a) The mean bias and (b) standard deviations of the bias PDFs in statistically homogeneous, clustered rain as functions of the ratio of the separation distance between successive, statistically independent samples (Δ) and the beam dimension B for $\chi_t = 2$ and N near unity when the number of independent samples per estimate is kept fixed at 10.

ally increase so that for a fixed L , there would actually be a reduction in the number of independent samples.

To illustrate, Fig. 8 is a plot of the results for the same situation as Fig. 7 except that the number of independent samples now decreases with increasing Δ/B because of, say, increasing antenna rotation rate. Obviously, the effects, which are now the combination of clustering and a reduction in the number of independent samples, can become quite substantial. [Note that while σ for the log and linear receivers actually decreases as Δ/B increases in Figs. 7b and 8b, the average biases (Figs. 7a and 8a) are changing as well so that even for

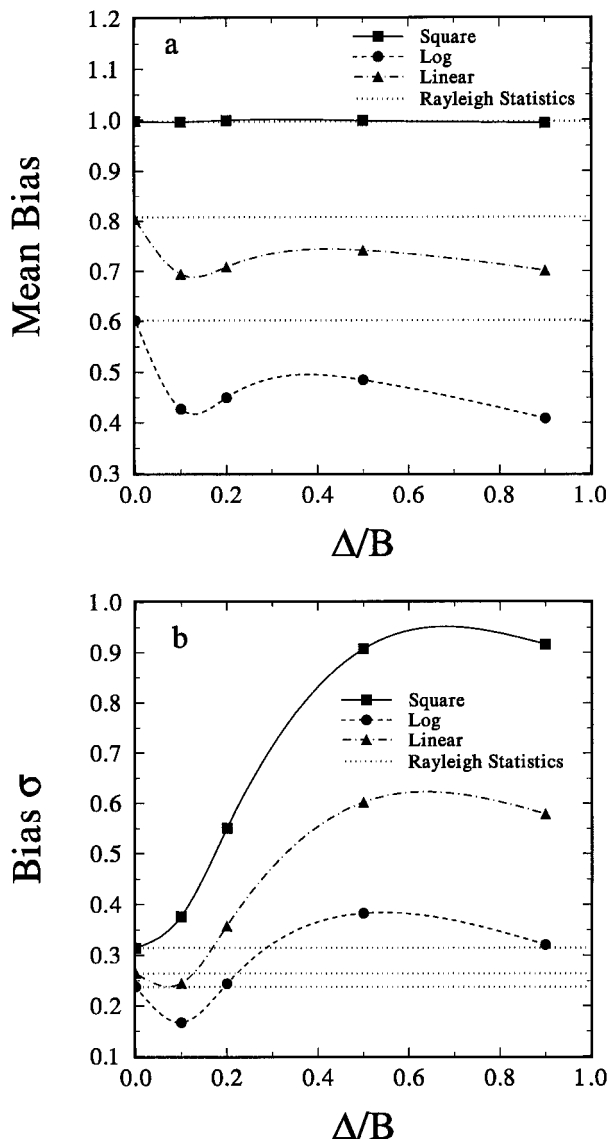


FIG. 8. Similar to Fig. 7 except that the number of independent samples varies as a function of Δ/B , as discussed in the text.

these receivers, the potential for error during measurements is enhanced as Δ/B increases.]

Now in all the calculations above, B is kept constant at 10. However, for the same rain field, Figs. 7 and 8 can be used to illustrate what happens as B decreases. If the interval between independent samples is maintained as B shrinks, then Δ/B would obviously increase along a curve similar to one of those in Fig. 7.

However, there is often a constraint to cover some distance \mathcal{L} , consisting of several estimate distances L , in a fixed time \mathcal{T} . (One example, for instance, might be to insist on a complete volume scan every 8 min, say.) If, for smaller B , the scan rate is increased to cover \mathcal{L} in time \mathcal{T} , then Δ increases (and, of course, Δ/B increases). Consequently, the tendency is for the number

of independent samples per estimate to decrease, and the appropriate curve is then more like one of those in Fig. 8. Furthermore, because the beam filtering of fluctuations is less effective the smaller the beam as discussed above, non-Rayleigh deviations are likely to be more enhanced for smaller B . Hence, in that sense smaller beams will usually tend to see larger fluctuations than larger beams and, therefore, may be more influenced by non-Rayleigh effects.

On the other hand, it is not too difficult to generate scenarios in which Δ/B may become quite large even for broad beams. Hence, in general to minimize non-Rayleigh effects it is best to keep $\Delta/B \ll 1$. In addition, to reduce the influence of χ_t , it is best to keep L as small as possible in an attempt approach the condition that $\chi_t/L > 1$ (Fig. 5). The first condition can be achieved most readily using signal whitening (Schulz and Kostinski 1997; Koivunen and Kostinski 1999) or by implementing frequency chirp. The second condition may be addressed using these same techniques as well and by holding the beam nearly stationary while forming an estimate. A good example of the latter approach is the use of electronic antenna steering by spaceborne remote sensing instruments in which the observation volume is held nearly stationary during measurements even as the satellite moves.

4. Summary and remarks

This study shows that even in a statistically homogeneous rain field, the clustering of raindrops can lead to biases enhanced beyond values expected assuming Rayleigh statistics. This result could not have been deduced in any of the previous work on non-Rayleigh signal statistics (Rogers 1971; Scarchilli et al. 1986; Jameson and Kostinski 1996; Awaka and Iguchi 1997). It is only because of recent advances in our understanding of the natural structure of rain (Kostinski and Jameson 1997; Jameson and Kostinski 1998; Kostinski and Jameson 1999; Jameson et al. 1999) that we can now identify such effects. Yet, this finding may be significant since even in fairly uniform-looking fields of reflectivity factor, some non-Rayleigh effects may still lurk. Furthermore, these effects of clustering are likely to be enhanced, sometimes considerably, by statistically inhomogeneous rain fields because of the greatly increased variance associated with such fields (see Jameson and Kostinski 1996).

It is also now clear that the magnitude of the non-Rayleigh effects even in statistically homogeneous rain depend upon the two different factors, namely the *intrinsic spatial structure of the rain* as characterized by χ_t and \mathfrak{K} as well as the *geometry of the observations* as specified by Δ , L , and B . Since χ_t is not generally known, reductions in potential non-Rayleigh effects must be achieved by minimizing Δ and L using techniques such as hold and sample, chirping, and signal whitening. The Δ/B should also be kept to values $\ll 1$.

It is not recommended to scan an antenna as rapidly as possible in order to gather measurements over some prescribed volume under a time constraint that may lead to violations of either of these two conditions.

It is also worth mentioning that in all of this discussion and in these Monte Carlo experiments, each sample is independent so that Δ actually represents the incremental distance between *independent* samples. For most radars and other remote sensors, however, successive samples are often highly correlated. For such correlated samples, then, it may only be every fifth or tenth value that is independent. In such rather typical cases, correlated samples effectively increase Δ/B thereby enhancing the likelihood and the magnitude of non-Rayleigh effects. It is already quite clear that those radars such as NEXRAD that lack chirp or signal whitening, for example, are likely to experience significantly more non-Rayleigh deviations than are radars equipped to ensure the independence of each sample even in statistically homogeneous rain.

Even without these techniques, data can still be monitored for non-Rayleigh effects. One of the insidious aspects of non-Rayleigh signal statistics is that at times even though the data may look "perfectly normal," it may actually deviate considerably from the intrinsic "true" values that one strives to measure, that is, an estimate may be biased or may be very uncertain (large σ). While perhaps of less concern for qualitative observations, the increasing use of radar for more quantitative applications such as rainfall measurement may require monitoring of the data for non-Rayleigh effects. Yet many such deviations, while important, are likely to remain invisible even to trained observers. Fortunately, however, there are processing methods for monitoring the data (Jameson and Kostinski 1996).

Finally, it is worth mentioning again that besides rain, non-Rayleigh statistics can be expected to affect observations by many instruments other than radar whenever samples are collected while scanning across variable conditions. These include observations by radiometers, scatterometers, and lidars.

Acknowledgments. This work was supported by the National Science Foundation under Grants ATM95-12685 (AK), ATM94-19523 (AJ), ATM97-08657 (AJ), and ATM97-12075 (AJ).

REFERENCES

- Awaka, J., and T. Iguchi, 1997: On averages of radar rain echoes in nonstationary conditions. *IEEE Trans. Geosci. Remote Sens.*, **35**, 1094–1104.
- Doviak, R. J., and D. S. Zrnić, 1993: *Doppler Radars and Weather Observations*. Academic Press, 562 pp.
- Evans, M., N. Hastings, and B. Peacock, 1993: *Statistical Distributions*. John Wiley and Sons, 170 pp.
- Feller, W., 1968: *An Introduction to Probability Theory and Its Application*. Vol. 2. John Wiley and Sons, 509 pp.
- Jameson, A. R., and A. B. Kostinski, 1996: Non-Rayleigh signal

- statistics caused by relative motion during measurement. *J. Appl. Meteor.*, **35**, 1846–1859.
- , and —, 1998: Fluctuation properties of precipitation. Part II: Reconsideration of the meaning and measurement of raindrop size distributions. *J. Atmos. Sci.*, **55**, 283–294.
- , —, and A. Kruger, 1999: Fluctuation properties of precipitation. Part IV: Finescale clustering of drops in variable rain. *J. Atmos. Sci.*, **56**, 82–91.
- Johnson, G. E., 1994: Constructions of particular random processes. *Proc. IEEE*, **82**, 270–285.
- Koivunen, A. C., and A. B. Kostinski, 1999: The feasibility of data whitening to improve performance of a Doppler weather radar. *J. Appl. Meteor.*, in press.
- Kostinski, A. B., and A. R. Jameson, 1997: Fluctuation properties of precipitation. Part I: Deviations from the Poisson distribution in precipitation. *J. Atmos. Sci.*, **54**, 2174–2186.
- , and —, 1999: Fluctuation properties of precipitation. Part III: The ubiquity and emergence of the exponential drop size spectra. *J. Atmos. Sci.*, **56**, 111–121.
- Marshall, J. S., and W. Hitschfeld, 1953: Interpretation of the fluctuating echo from randomly distributed scatterers. Part I. *Can. J. Phys.*, **31**, 962–994.
- Rayleigh, S., 1877: *The Theory of Sound*. Vol. 1. Reprint, Dover Publications, 1945, 984 pp.
- Rogers, R. R., 1971: The effect of variable target reflectivity on weather radar measurements. *Quart. J. Roy. Meteor. Soc.*, **97**, 154–167.
- Scarchilli, G., E. Gorgucci, and R. Leonardi, 1986: Theory and optimization of the excess bias measurement. *J. Atmos. Oceanic Technol.*, **3**, 217–229.
- Schaffner, M. R., R. Rinehart, and R. Leonardi, 1980: Detection of nonuniformities within the radar measurement cell. Preprints, *19th Conf. on Radar Meteorology*, Miami, FL, Amer. Meteor. Soc., 256–263.
- , R. Carbone, and E. Gorgucci, 1983: Information from bias measurements. Preprints, *20th Conf. on Radar Meteorology*, Edmonton, SK, Canada, Amer. Meteor. Soc., 523–528.
- Schulz, T., and A. B. Kostinski, 1997: Variance bounds on the estimation of intensity and polarimetric parameters in radar meteorology. *IEEE Trans. Geosci. Remote Sens.*, **35**, 248–255.